https://ntrs.nasa.gov/search.jsp?R=20090026596 2019-08-30T07:34:18+00:00Z

Heavy Ion Microbeam and Broadbeam Transients in SiGe HBTs

Jonathan A. Pellish, Robert A. Reed, Dale McMorrow, Gyorgy Vizkelethy, Veronique Ferlet-Cavrois, Jacques Baggio, Philippe Paillet, Olivier Duhamel, Stanley D. Phillips, Akil K. Sutton, Ryan M. Diestelhorst, John D. Cressler, Paul E. Dodd, Michael L. Alles, Ronald D. Schrimpf, Paul W. Marshall, and Kenneth A. LaBel

Abstract

SiGe HBT heavy ion current transients are measured using microbeam and both high- and low-energy broadbeam sources. These new data provide detailed insight into the effects of ion range, LET, and strike location.

Corresponding and Presenting Author

- J. A. Pellish is with the NASA Goddard Space Flight Center, Code 561.4, 8800 Greenbelt RD, Greenbelt, MD 20771 USA. Phone: 301.286.6523, Fax: 301.286.4699, Email: jonathan.a.pellish@nasa.gov

Contributing Authors

- R. A. Reed, M. L. Alles and R. D. Schrimpf are with the Department of Electrical Engineering and Computer Science, Vanderbilt University, 2301 Vanderbilt PL, Station B 351824, Nashville, TN 37235 USA.
- D. McMorrow is with the Naval Research Laboratory Code 6812, 4555 Overlook AVE, SW, Washington, DC 20375 USA.
- G. Vizkelethy and P. E. Dodd are with Sandia National Laboratories, Albuquerque, NM 87185 USA.
- V. Ferlet-Cavrois, J. Baggio, P. Paillet, and O. Duhamel are with the CEA, DAM, DIF, F-91297 Arpajon, France.
- S. D. Phillips, A. K. Sutton, R. M. Diestelhorst, and J. D. Cressler are with the School of Electrical and Computer Engineering, Georgia Institute of Technology, 777 Atlantic DR, NW, Atlanta, GA 30332 USA.
- P. W. Marshall is a NASA consultant, Brookneal, VA 24528 USA.
- K. A. LaBel is with the NASA Goddard Space Flight Center, Code 561.4, 8800 Greenbelt RD, Greenbelt, MD 20771 USA.

Session Preference: Single-Event Effects, Mechanisms and Modeling
Presentation Format: Oral

This work was supported in part by the NASA Electronic Parts and Packaging Program, the Defense Threat Reduction Agency Radiation Hardened Microelectronics Program under *IACRO* #09-4587I to NASA, the Georgia Electronic Design Center, the Naval Research Laboratory, the Commissariat à l'Énergie Atomique, an AFOSR DURIP to Vanderbilt University, and Sandia National Laboratories. Sandia is a multi-program laboratory operated by Sandia Corporation, a Lockheed Martin Company, for the United States Department of Energy's National Nuclear Security Administration under Contract DE-AC04-94AL85000. The authors thank Ari Virtanen, Arto Javanainen, and the RADEF team at the University of Jyväskylä, Finland for the heavy ion beam time. The authors also thank Stéphane Guillous, Jean-Marc Ramillon, and the management team at GANIL in Caen, France for access to the high-energy xenon beam time. The authors also extend thanks Lewis Cohn, Maj. James Fee, and the SiGe team at IBM for their ongoing support.

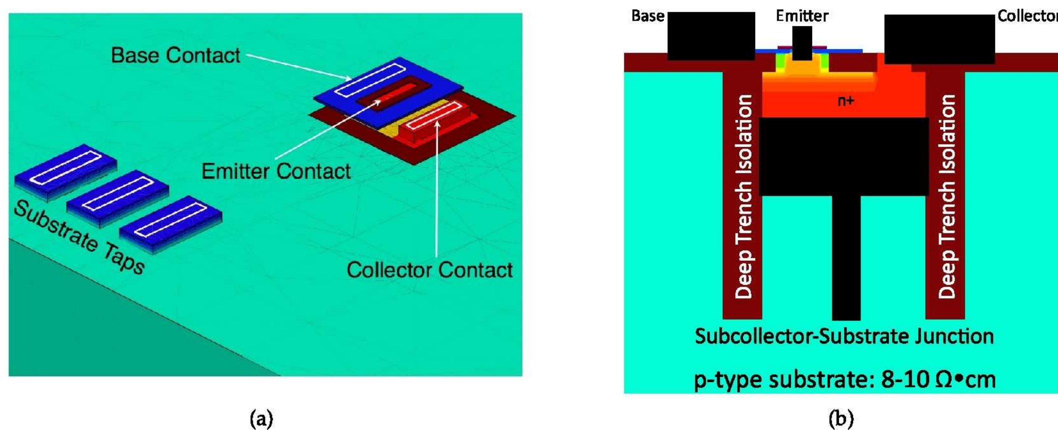

(a) (b)

Fig. 1: 3-D and 2-D renderings of the device under test for the heavy ion experiments. **(a)** shows a 3-D model of an npn IBM 5AM SiGe HBT with emitter area $A_E = 0.5 \times 2.5\ \mu m^2$. The 3-D geometry was extracted from the GDSII file of the test structures. **(b)** shows a 2-D slice through the short dimension of the device (emitter width) shown in **(a)**. Note the deep trench isolation, subcollector-substrate junction, and the lightly-doped p-type substrate. The deep trench isolation is approximately 7 μm in length, 1 μm thick, and has inner dimensions of $4.1 \times 4.3\ \mu m^2$.

1 Introduction

High-reliability applications designed for use in space may employ silicon-germanium heterojunction bipolar transistors (SiGe HBTs), like the one shown in Fig. 1, because they offer both performance and total ionizing dose (TID) benefits over standard silicon CMOS processes while still allowing monolithic fabrication [1,2]. The majority of SiGe HBT applications tested within the radiation effects community have been high-speed serial shift registers [3–7]. Because the data rates of these circuits regularly exceed 1 Gbit/s, the detailed characteristics of ion-induced current transients become important and are necessary for a full understanding of behavior in a particular radiation environment [8–10].

The heavy ion microbeam position-correlated data, coupled with a range of broadbeam energies and linear energy tranfers (LETs), provide a unique and detailed perspective on the temporal profile of ion-induced currents in this important semiconductor technology. These results are consistent with previous pulsed-laser measurements [11] as well as broadbeam data conclusions, including those regarding cross section effects at low LET and grazing angles [3–5, 12]. The different LETs and particle energies show the consequences of heavy ion charge generation and collection in devices with lightly-doped substrates. These data capture essential missing information required for accurate device physics modeling.

2 Experimental Details and Results

Single event current transients were collected at three different facilities: Sandia National Laboratories' ion microbeam (SNL), the University of Jyväskylä (JYFL), and the Grand Accélérateur National d'Ions Lourds (GANIL). The data gathered at SNL are based on 36 MeV ^{16}O and include the xy-coordinates of each ion strike. The data collected at JYFL and GANIL are broadbeam data, gathered without knowledge of ion strike location, but possess higher energy, the possibility of angled irradiation, and a wide selection of LETs. JYFL heavy ion exposures included 9.3 MeV/u ^{20}Ne, ^{40}Ar, ^{82}Kr, and ^{131}Xe. The ^{40}Ar irradiations were performed at a tilt of 60° in addition to normal incidence. All other exposures were completed at normal incidence only. GANIL irradiations were performed at normal incidence with 45.5 MeV/u ^{136}Xe.

The device under test (DUT) is an IBM 5AM SiGe HBT with emitter area $A_E = 0.5 \times 2.5\ \mu m^2$ and inner deep trench isolation dimensions of $4.1 \times 4.3\,\mu m^2$, shown in Fig. 1. It was mounted in a custom high-speed package with four 2.9 mm coaxial bulkhead connectors joined to microstrip transmission lines. The DUT was wire bonded to the microstrips using 1 mil gold wire; details of this setup are described elsewhere [11]. At JYFL and GANIL, the transients on the base and collector were measured and recorded with a Tektronix DPO71604A 16 GHz (40 GS/s), real-time digital phosphor oscilloscope (DPO). At SNL, substrate, collector, base, and emitter transients were measured and recorded with a Tektronix DPO72004 20 GHz (50 GS/s), real-time DPO. The experiments focused on three bias conditions for the DUT: **(Case 1)** $V_{Sub} = -4$ V, **(Case 2)** $V_C = 3$ V, and **(Case 3)** $V_{Sub} = -3$ V. If the terminal is not listed, it is grounded.

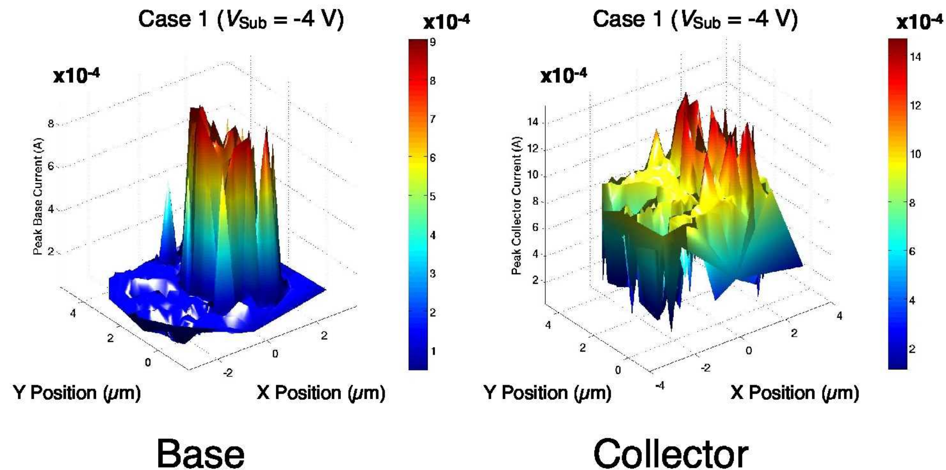

(a) IBM 5AM SiGe HBT, $A_E = 0.5 \times 2.5\ \mu m^2$ emitter area, and inner deep trench isolation dimensions of $4.1 \times 4.3\,\mu m^2$

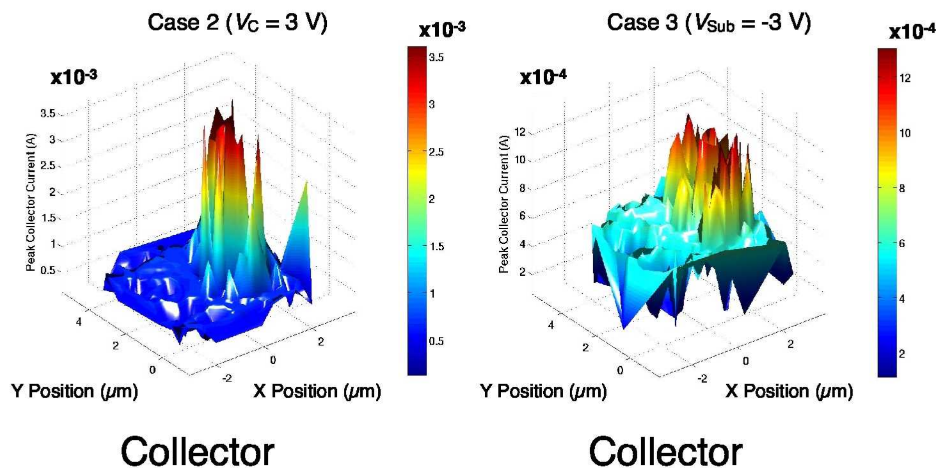

(b) IBM 5AM SiGe HBT, $A_E = 0.5 \times 2.5\ \mu m^2$ emitter area, and inner deep trench isolation dimensions of $4.1 \times 4.3\,\mu m^2$

Fig. 2: 36 MeV ^{16}O TRIBIC scan on an IBM 5AM SiGe HBT with **(a)** $V_{Sub} = -4$ V (Case 1) and **(b)** $V_C = 3$ V (Case 2) and $V_{Sub} = -3$ V (Case 3). If the bias is not given, the terminal is grounded. The peak current for the collector and base terminals is plotted. The collector transients were scaled by -1 to yield a positive scale. Also note that the data sets have different ordinate scales. The jagged surface in the data is due to the delaunization algorithm's interpretation of the irregular xy-spacing.

Figs. 2(a) and 2(b) plot the peak base and collector currents as a function of position obtained from a 36 MeV ^{16}O time-resolved ion beam-induced charge (TRIBIC) [13] scan on an IBM 5AM SiGe HBT for the base and collector terminals under the three different bias conditions previously described. The scan area is 20 μm by 20 μm with 200 nm steps and a spatial resolution of $< 1\ \mu$m. The scans produced around 400 data points based on a -4 mV trigger on the collector. As was observed in previous laser testing results [11], the peak collector responses are confined to the base-collector junction, which is located on the y-axis between 0 and 4 μm and between 0 and 2 μm on the x-axis. Since the triggers are confined to the deep trench isolation area, and base transients of Fig. 2(a) entirely to the base-collector junction, this enables position correlation of the broadbeam strikes in reference to the DUT's physical structures.

In Fig. 2(b), with a large positive bias on the collector (Case 2) instead of a negative bias on the substrate (Cases 1 and 3), the collector current transients within the base-collector junction are magnified by more

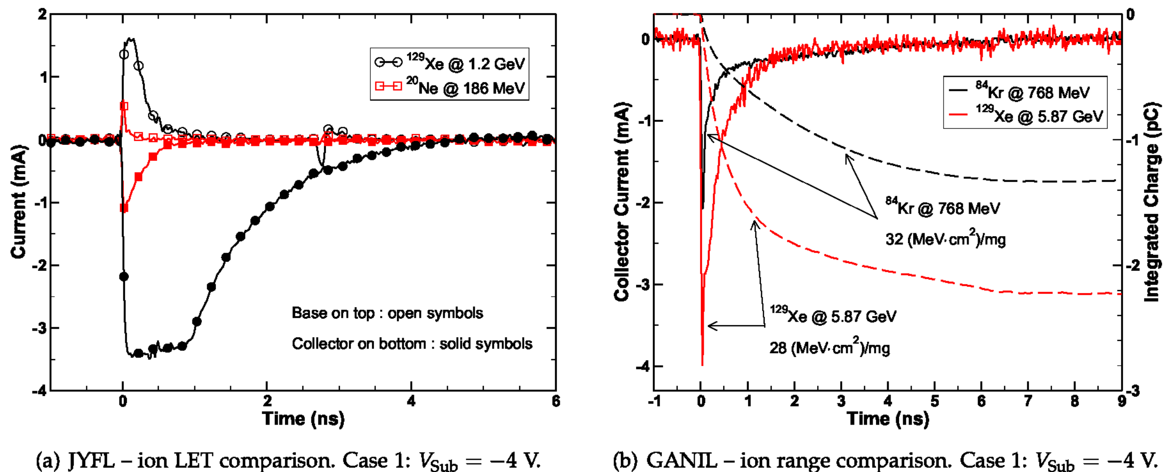

(a) JYFL – ion LET comparison. Case 1: $V_{\text{Sub}} = -4$ V.

(b) GANIL – ion range comparison. Case 1: $V_{\text{Sub}} = -4$ V.

Fig. 3: **(a)** shows neon and xenon transients captured at JYFL demonstrating device response to two extreme LETs, 3.7 $(\text{MeV}\cdot\text{cm}^2)/\text{mg}$ for the neon ions and 60 $(\text{MeV}\cdot\text{cm}^2)/\text{mg}$ for the xenon ions; the integrated charge is labeled next to each curve. The neon transients are similar to those measured with the SNL microbeam. **(b)** shows a 45.5 MeV/u xenon transient measured at GANIL compared to a 9.3 MeV/u krypton transient measured at JYFL. Though the two ions have similar LETs, they produce different transients and integrated charges.

than a factor of two. The rest of the area within the deep trench isolation shows transients of approximately the same peak magnitude at 0.5 mA (Cases 2 and 3), which occurs because the same potential is dropped across the subcollector/substrate junction. The magnification of the base-collector junction transients in Case 2 is due to a combination of the Early effect and avalanche multiplication [11].

A good representation of the JYFL broadbeam heavy ion results is shown in Fig. 3(a), which demonstrates the significance of ion LET on the production of current transients. Based on knowledge of the microbeam data already presented, the transients shown in Fig. 3(a) are the result of direct hits to the active region of the device; each pair shown are correlated events from a single ion. The average neon transient had a peak magnitude of 0.25 ± 0.04 mA (base) and 0.90 ± 0.04 mA (collector). For xenon, the average peak magnitudes are 0.57 ± 0.08 mA (base) and 2.9 ± 0.19 mA (collector). These transients were captured with a -15 mV trigger on the collector terminal, which is larger than the trigger used at SNL due to electrical noise encountered at the JYFL facility. A lower trigger value would have resulted in more captured transients, and perhaps measurement of transients originating from strikes outside the deep trench isolation; however, these events are difficult to measure. Single-event current transients for strikes outside the deep trench are best handled with calibrated 3-D technology computer aided design, which will appear in the final paper.

As expected, the xenon transient in Fig. 2(a) produces more charge that yields large transients on both the collector and base terminals. The plateau in the xenon collector transient, and large amount of collected charge, is due to the fact that the device terminals are tied to ideal voltage sources that can supply as much current as needed to maintain the terminal voltage. If the device had been connected to potential that would collapse under high current draw, the plateau and the transient would be shorter. The neon transients are similar to the SNL microbeam transients in Fig. 2(b) and compare well to previous pulsed laser testing [11]. The shape, duration, and contributing mechanisms of these transients will be investigated in the final paper with further data analysis and device simulations.

The JYFL argon testing at normal incidence and a 60° tilt confirmed that irradiating SiGe HBTs at angle produces fewer transients, based on an oscilloscope trigger value of -15 mV on the collector. At normal incidence with -4 V on the substrate, the oscilloscope captured 50 transients after a fluence of $3.85 \times 10^7\,\text{cm}^{-2}$. However, at a tilt of 60° with the same bias conditions, only 16 events were measured after a fluence of $1.94 \times 10^8\,\text{cm}^{-2}$, a 16$x$ decrease in cross section. This result confirms, at the device-level, the effect of cross-section decrease with increasing ion angle for low LET particles, observed in many previous broadbeam tests of SiGe HBT circuit applications [3–5]. It is critical to understand this effect in order to calculate event rates for space-based applications. Though the data are not presented here, they will be explored in more detail for the final paper.

The issue of ion range in the substrate, below the active region, is important for devices fabricated directly on lightly-doped substrates, such as SiGe HBTs and other bipolar devices. This is a key point for space applications, which will be the target of a variety of long-range heavy ions. Fig. 3(b) compares the current transients induced by two different particles with approximately the same LET, but different ranges. The 9.3 MeV/u ^{82}Kr ion has a range of approximately 90 μm in the substrate and the 45.5 MeV/u ^{136}Xe ion has a range of approximately 640 μm in the substrate, accounting for a maximum of 15 μm of overburden. For the krypton strike, the device collects approximately 5.0% of the total 27 pC of generated charge. In the case of xenon, the device collects about 2.3% of the 96 pC generated by the ion assuming a 300 μm substrate. However, comparing the two values of collected charge in Fig. 3(b) shows that the xenon strike results in almost a $2x$ increase. The average collector peak magnitude current for 45.5 MeV/u xenon strikes to the DUT is 1.6 ± 0.06 mA – compared to krypton at 0.81 ± 0.15 mA. While the krypton and xenon collector current transients in Fig. 3(b) are both large compared to their averages, the $2x$ increase in collected charge is still supported by the peak current magnitude averages assuming that peak current is proportional to collected charge.

The additional xenon collected charge in Fig. 3(b) occurs over a short period of time indicating that it is related to the equipotential deformation of the subcollector junction depletion region [11]. Since the tail of each transient is coincident past about 1.5 ns, the charge collection is not related to diffusion transport. This implies that the long range of the high-energy xenon ion causes a more substantial deformation of the subcollector depletion region resulting in greater charge collection.

3 Conclusion

These heavy ion current transient data represent a significant improvement to the state-of-the-art understanding of heavy ion-induced charge in SiGe HBTs. These results, when combined with 3-D technology computer-aided design simulations in the final paper, will finally complete previous heavy ion microbeam and pulsed laser data sets. Previous microbeam data [14] only measured collected charge and previous two-photon pulsed-laser transient measurements [11] cannot be easily correlated to ion LET and ion-specific effects. Taken as a whole and coupled with device simulation, a complete picture of charge generation, transport, and collection in bulk SiGe HBTs is possible.

References

[1] J. D. Cressler, Ed., *The Silicon Heterostructure Handbook: materials, fabrication, devices, circuits, and applications of SiGe and Si strained-layer epitaxy*. Boca Raton, FL: CRC, 2006.

[2] J. D. Cressler, "SiGe BiCMOS technology: an IC design platform for extreme environment electronics applications," in 45th *Annu. Int. Reliability Physics Symp.* Phoenix, AZ: IEEE, Apr. 2007, pp. 141–149.

[3] P. W. Marshall *et al.*, "Single event effects in circuit-hardened SiGe HBT logic at gigabit per second data rates," *IEEE Trans. Nucl. Sci.*, vol. 47, no. 6, pp. 2669–2674, Dec. 2000.

[4] R. A. Reed *et al.*, "Heavy-ion broad-beam and microprobe studies of single-event upsets in 0.20 μm SiGe heterojunction bipolar transistors and circuits," *IEEE Trans. Nucl. Sci.*, vol. 50, no. 6, pp. 2184–2190, Dec. 2003.

[5] P. W. Marshall *et al.*, "Autonomous bit error rate testing at multi-gbit/s rates implemented in a 5AM SiGe circuit for radiation effects self test (CREST)," *IEEE Trans. Nucl. Sci.*, vol. 52, no. 6, pp. 2446–2454, Dec. 2005.

[6] R. Krithivasan *et al.*, "Application of RHBD techniques to SEU hardening of third-generation SiGe HBT logic circuits," *IEEE Trans. Nucl. Sci.*, vol. 53, no. 6, pp. 3400–3407, Dec. 2006.

[7] A. K. Sutton *et al.*, "Proton-induced SEU in SiGe digital logic at cryogenic temperatures," *Solid State Electron.*, vol. 52, no. 10, pp. 1652–1659, Oct. 2008.

[8] G. Niu *et al.*, "Simulation of SEE-induced charge collection in UHV/CVD SiGe HBTs," *IEEE Trans. Nucl. Sci.*, vol. 47, no. 6, pp. 2682–2689, Dec. 2000.

[9] ——, "Modeling of single-event effects in circuit-hardened high-speed SiGe HBT logic," *IEEE Trans. Nucl. Sci.*, vol. 48, no. 6, pp. 1849–1854, Dec. 2001.

[10] X. Wei *et al.*, "3-D mixed-mode simulation of single event transients in SiGe HBT emitter followers and resultant hardening guidelines," *IEEE Trans. Nucl. Sci.*, vol. 55, no. 6, pp. 3360–3366, Dec. 2008.

[11] J. A. Pellish *et al.*, "Laser-induced current transients in silicon-germanium HBTs," *IEEE Trans. Nucl. Sci.*, vol. 55, no. 6, pp. 2936–2942, Dec. 2008.

[12] ——, "A generalized SiGe HBT single-event effects model for on-orbit event rate calculations," *IEEE Trans. Nucl. Sci.*, vol. 54, no. 6, pp. 2322–2329, Dec. 2007.

[13] M. B. H. Breese *et al.*, "A review of ion beam induced charge microscopy," *Nucl. Instr. and Meth. B*, vol. 264, no. 2, pp. 345–360, Nov. 2007.

[14] J. A. Pellish *et al.*, "Substrate engineering concepts to mitigate charge collection in deep trench isolation technologies," *IEEE Trans. Nucl. Sci.*, vol. 53, no. 6, pp. 3298–3305, Dec. 2006.